Investigation of diffusion kinetics of plasma paste borided AISI 8620 steel using a mixture of B_2O_3 paste and B_4C/SiC

IBRAHIM GUNES[a,*], SUKRU TAKTAK[a], CUMA BINDAL[b], YILMAZ YALCIN[a], SUKRU ULKER[a] and YUSUF KAYALI[a]

[a]Technology Faculty, Afyon Kocatepe University, 03200, Afyonkarahisar, Turkey
[b]Faculty of Engineering, Sakarya University, Sakarya, Turkey
e-mail: igunes@aku.edu.tr

Abstract. In the present study, AISI 8620 steel was plasma paste borided by using various B_2O_3 paste mixture. The plasma paste boriding process was carried out in a dc plasma system at temperatures of 973, 1023 and 1073 K for 2, 5 and 7 h in a gas mixture of 70% H_2 -30% Ar under a constant pressure of 10 mbar. The properties of the boride layer were evaluated by optical microscopy, X-ray diffraction, Vickers micro-hardness tester and the growth kinetics of the boride layers. X-ray diffraction analysis of boride layers on the surface of the steel revealed FeB and Fe_2B phases. Depending on temperature and layer thickness, the activation energies of boron in steel were found to be 124.7 kJ/mol for 100% B_2O_3.

Keywords. Plasma paste boriding; AISI 8620; B_2O_3 paste; kinetics; activation energy.

1. Introduction

Boriding is a thermo-chemical treatment that diffuses boron through the surface of metallic substrates. As boron is an element of relatively small size it diffuses into a variety of metals; including ferrous, non-ferrous and some super alloys (Torun & Celikyurek 2009; Lou *et al* 2009; Dong *et al* 2010). Thermal diffusion treatments of boron compounds used to form iron borides typically require process temperatures of 973–1273 K in either gaseous, solid (Yu *et al* 2005), salt media (Bindal & Ucisik 1999), ion implanting (Shrivastava *et al* 1996), spark plasma sintering (SPS) (Yu *et al* 2002), electrochemical (Kartal *et al* 2011), plasma-electrolysis (Bejar & Henríquez 2009), plasma boriding (Rodríguez *et al* 1999) and plasma paste boriding (Gunes *et al* 2011; Yoon *et al* 1999; Ulker *et al* 2011).

In order to decrease the boriding temperature and time, ion implantation boriding (Buijnsters *et al* 2003), and plasma-assisted boriding (Khor *et al* 2005) have been studied over the past 40 years (Davis *et al* 1998; Yan *et al* 2002). Although the plasma boriding process has a superior advantage when compared to conventional boriding processes, the gases (B_2H_6, BCl_3) used in plasma boriding, which have expensive, poisonous and explosive characteristics, making it as

disadvantageous. The disadvantages in the plasma boriding process can be eliminated through the plasma paste boriding surface process. The fact that the paste used has environmentally friendly boron raw materials and that the gases used are generally hydrogen, argon and nitrogen, which have inert characteristics, make this process advantageous. Yoon *et al* (1999), who studied plasma paste boriding of AISI 304 steel, reported that using the plasma paste process caused lower activation energy for the formation of the boride layer than that of conventional boriding processes. Gunes *et al* (2011) carried out plasma paste boriding of AISI 52100, 8620 and 440C steels by using 100% borax paste. This work indicated that a thicker boride layer was formed than when using conventional boriding methods at similar temperatures.

There is scanty literature about the characterization of paste borided steels in a plasma environment. In this study, low alloyed AISI 8620 steel was plasma paste borided. The main objective of this study was to characterize plasma paste borided AISI 8620 steel using B_2O_3 based pastes. The phase structure, microhardness and diffusion kinetics of the boride layers were investigated using X-ray diffraction (XRD), microhardness tester and Arrhenious equation.

2. Experimental

The substrate material, AISI 8620, essentially contained: 0.19 wt.% C, 0.4 wt.% Cr, 0.7 wt.% Mn, 0.4 wt.% Ni steel. The samples had a cylindrical shape and were 18 mm in diameter and 6 mm in length. AISI 8620 steel samples were ground using 1000 mesh SiC paper and polished with 0.1 alumina suspension to obtain a smooth surface. In this study, B_2O_3, SiC and B_4C powder mixture at various percentages were used as a paste. The removal of the B_2O_3 paste remaining on the surface of the specimen borided with 100% B_2O_3 paste is difficult and the process is time-consuming, therefore, SiC and B_4C were added to the B_2O_3 paste. SiC and B_4C were also added as catalysts to the B_2O_3 paste. Figure 1 shows the flow chart of the preparation of boric acid based pastes on the sample steels for plasma paste boronizing. The powder mixtures
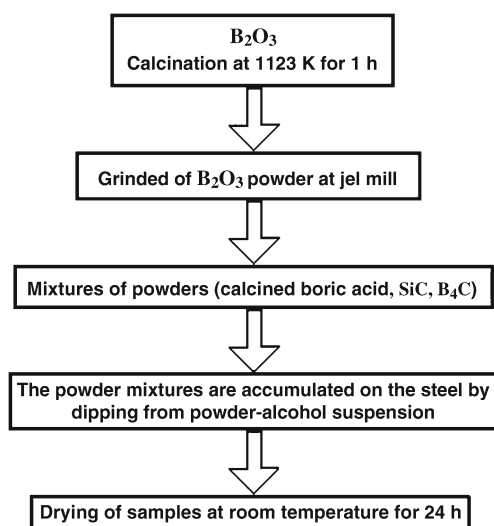
Figure 1. Flow chart of preparing of B_2O_3 based pastes on the samples steel for plasma paste boriding.

Table 1. Ratios of paste mixtures used for plasma paste boriding.

B_2O_3	SiC	B_4C
100%	——	——
70%	30%	——
70%	——	30%
30%	70%	——
30%	——	70%

were accumulated on the steel by dipping from a powder–alcohol suspension. Percentages of paste mixture used in this study are shown in table 1.

The plasma paste boriding treatment was performed in a dc plasma system, which is described in (Gunes *et al* 2011). The prepared samples were placed in a vacuum container and container pressure was set to 2×10^{-2} mbar of vacuum. The samples were plasma paste borided at 973, 1023 and 1073 K for 2, 5 and 7 h in a gas mixture of 70%H_2 - 30%Ar under a constant pressure of 10 mbar. The temperature of the samples was measured using a chromel–alumel thermocouple, placed at the bottom of the treated samples. After the plasma paste boride process, the remains of SiC and B_4C paste on each sample was cleaned in an ultrasonic bath with alcohol.

Cross-sections of plasma paste borided steels were prepared metallographically to observe morphological details using a BX60 Olympus microscope. The X-ray diffractograms were obtained using a copper tube source in the conventional bragg-brentano (θ-2θ) technique having symmetric geometry with monochromatized radiation (Cu Kα, $\lambda = 0.15418$ nm). The thickness of the layers formed on the steels was measured by an optical micrometer attached to the optical microscope.

The hardness of the boride layers was measured on the cross-sections using the Micro-Vickers indenter (Shimadzu HMV-2) with 50 g loads.

3. Result and discussion

3.1 *Surface characterization*

Figure 2 illustrates optical microstructures of plasma paste borided steel at 1023 K for 5 h for 100% B_2O_3, 70% B_2O_3 + 30% SiC, 70% B_2O_3 + 30% B_4C, 30% B_2O_3 + 70% SiC, 30% B_2O_3 + 70% B_4C paste mixture. The morphology of borides formed on the surface of the substrate has a columnar nature.

At the end of the plasma paste boriding treatment, boride layer thicknesses between 6 and 66 μm were obtained depending on boriding temperature and time. While the highest boron layer thickness was obtained for 100% B_2O_3, the lowest boron layer was obtained for 70% B_2O_3 + 30% B_4C paste mixture.

Yoon *et al* (1999) reported that using the plasma paste boriding method for stainless steel, a thick boride layer with a flat structure could be obtained in a shorter time and at a lower temperature than that obtained using conventional thermal diffusion, electrochemical, plasma-electrolysis and, spark plasma sintering (SPS) boriding (Yu *et al* 2002; Kartal *et al* 2011; Bejar & Henríquez 2009; Gunes *et al* 2011; Bartsch & Leonhardt 1999). Boriding processes at lower temperatures (973, 1023 and 1073 K) and in shorter time (2 h) can be performed by plasma paste boriding. This can be associated with plasma reducing the pollution of the environment (Nam *et al* 1998) and the activation energy required for the compound formation (Yoon *et al* 1999).
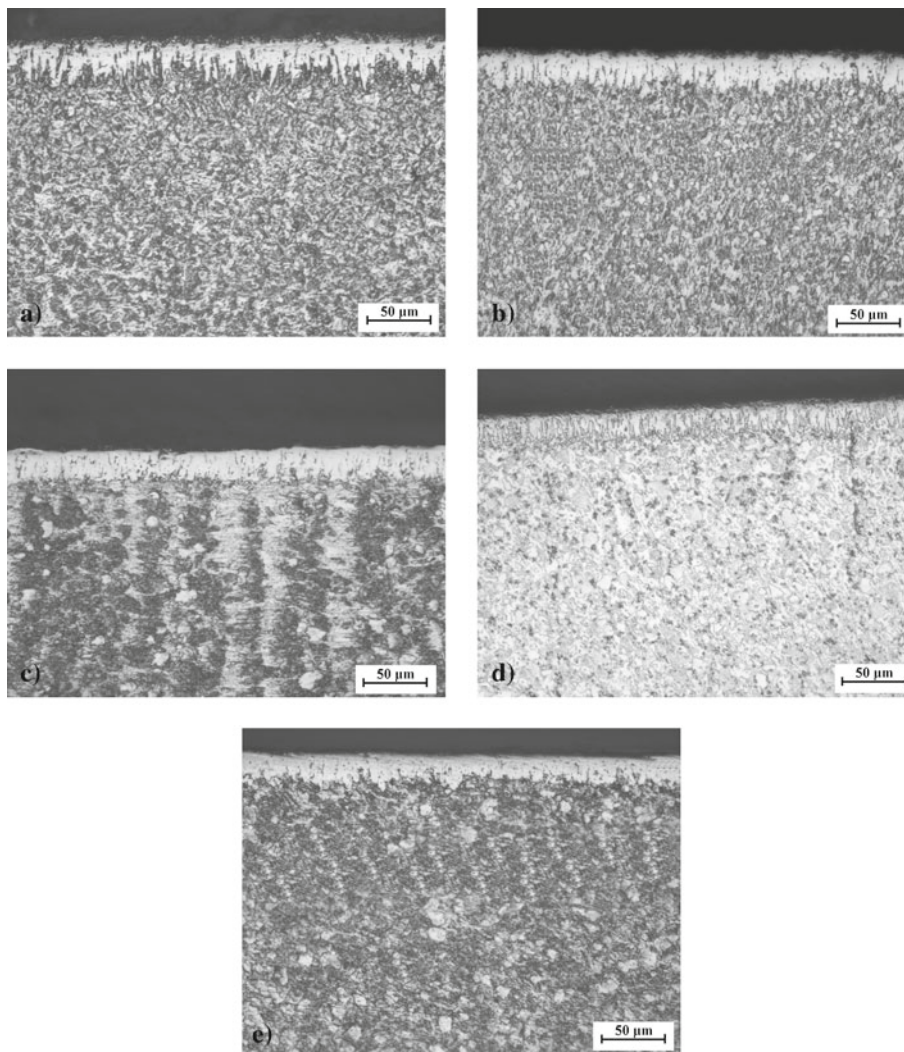
Figure 2. Optical cross-section microstructure of plasma paste borided steel in different % B_2O_3 paste mixtures for 5 h at 1023 K, **a**) 100 B_2O_3, **b**) 70 B_2O_3 + 30 SiC, **c**) 70 B_2O_3 + 30 B_4C, **d**) 30 B_2O_3 + 70 SiC, **e**) 30 B_2O_3 + 70 B_4C.

The X-ray diffraction (XRD) patterns of paste borided steel by plasma at various temperatures and times are given in figure 3. As seen in figure 3, for plasma paste borided steel, while an increase was observed in the FeB phase due to the plasma paste boriding temperature increase, a decrease occurred in the Fe_2B phase. The boride layers mainly consist of intermetallic phases (FeB and Fe_2B) as a result of diffusion of boron atoms from boriding compound to metallic lattice with respect to the holding time. The properties of these boride layers are known to a large extent by the help of these phases (Efe *et al* 2008; Kayali *et al* 2012). In the samples plasma paste borided with SiC added to B_2O_3 paste, the intensity of the Fe_2B phase was established to be slightly more dominant than the intensity of the FeB phase in figure 3. In the samples plasma paste borided with B_4C added to the B_2O_3 paste, the increase of the amount of B_4C also
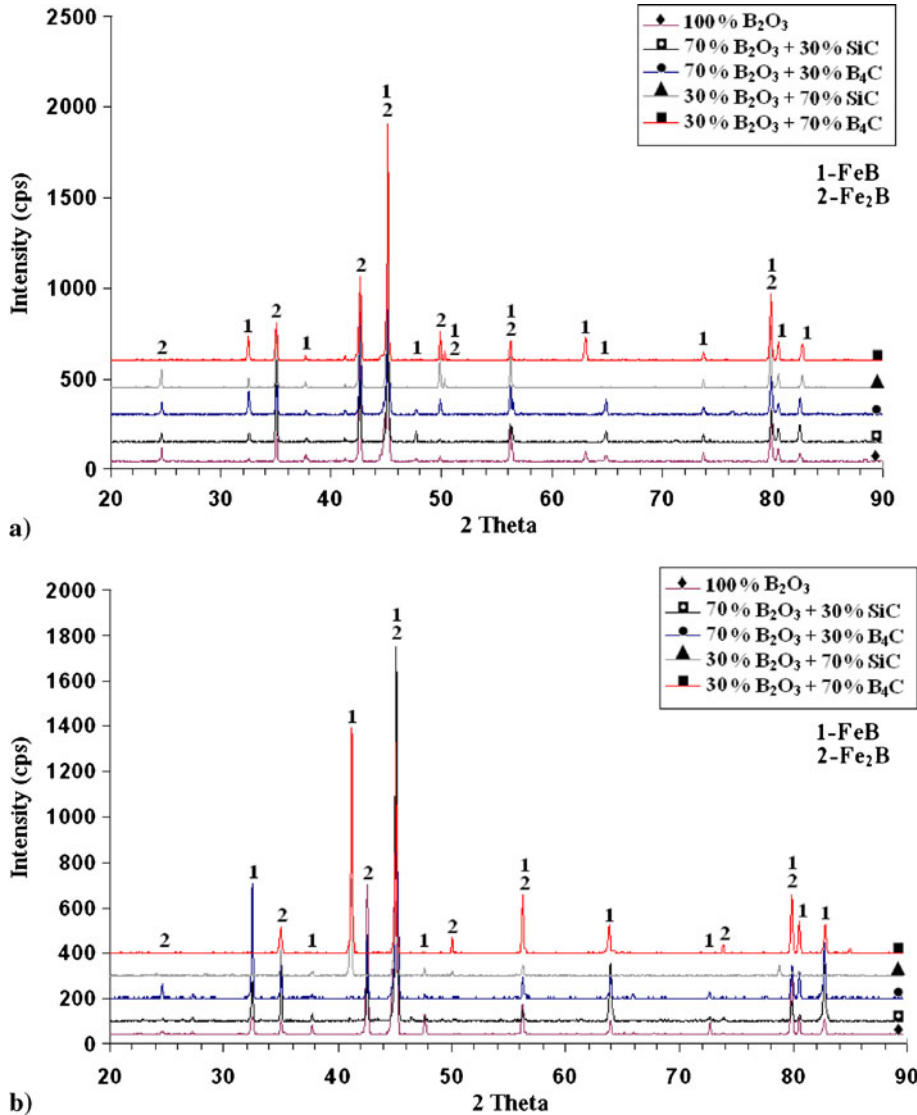
Figure 3. XRD patterns of the steel that was plasma paste borided for 5 h boronizing time and in different temperatures with different % B_2O_3 boron pastes, **a**) 973 K, **b**) 1073 K.

increased the phase intensity of FeB at the X-ray diffraction patterns in figure 3. During the once-through boriding process, when the boron concentration in the boriding media mixture (B_4C & SiC) depletes to a certain point, the chemical driving force is not high enough to incorporate the boron atoms into the FeB lattice, resulting in the consumption of the FeB phase to form the Fe_2B phase (Chen *et al* 2008).
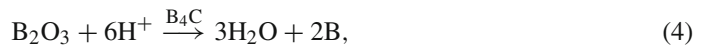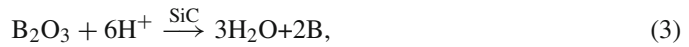
When the temperature of plasma is increased to about 1073 K, the B_2O_3 powders are firstly melted and then atomic boron is (B) formed. Atomic boron was produced through the decomposition of the boron hydride (BxHy) from the paste, and this atomic boron became the

active boron, B^{+1} within the molten B_2O_3 or in the glow discharge. Finally, this active boron, B^{+1}, diffused and reacted with Fe to form the boride layer (Gunes *et al* 2011).
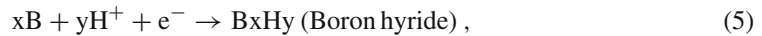
The reactions are exothermic and their Gibbs free energies can be calculated by the following formula (1):

$$\Delta_r G = \sum_{products} v\Delta_f G - \sum_{reactants} v\Delta_f G. \tag{1}$$

During plasma paste boriding, B_2O_3 reacts with active hydrogen (H^+) in glow discharge and the reaction occurs as follows

$$B_2O_3 + 6H^+ \rightarrow 3H_2O + 2B, \tag{2}$$

$$B_2O_3 + 6H^+ \xrightarrow{SiC} 3H_2O + 2B, \tag{3}$$

$$B_2O_3 + 6H^+ \xrightarrow{B_4C} 3H_2O + 2B, \tag{4}$$

$$\Delta G_B = -12.994 \text{ kcal}/\text{mol},$$

$$xB + yH^+ + e^- \rightarrow BxHy \text{ (Boron hyride)}, \tag{5}$$

$$BxHy \rightarrow xB + y/2H_2, \tag{6}$$

$$B^{+1} + 2Fe \rightarrow Fe_2B, \tag{7}$$

$$\Delta G_{Fe_2B} = -16.24 \text{ kcal}/\text{mol},$$

$$Fe_2B + B^{+1} \rightarrow 2FeB, \tag{8}$$

$$\Delta G_{FeB} = 9.124 \text{ kcal}/\text{mol}.$$

All the reactions can take place spontaneously and Gibbs free energies are under zero.

3.2 *Microhardness*

Figure 4 illustrates graphics showing hardness distributions of boride layers from surface to core belonging to AISI 8620 steel plasma paste borided in different B_2O_3% paste mixtures for 2, 5 and 7 h at 973, 1023 and 1073 K. Surface hardness appears to be high due to the FeB and Fe_2B phases formed as a result of the plasma paste boriding treatment. It is known that the FeB phase has higher than hardness values compared with Fe_2B phase (Sinha 1991; Sen *et al* 2001).

While the lowest hardness obtained was 1583 $HV_{0.05}$ for 70% B_2O_3 + 30% SiC boron paste mixture for 2 h at 973 K, the highest hardness was found for 30% B_2O_3 + 70% B_4C paste for 7 h at 1073 K at 1992 $HV_{0.05}$. Along with the increase in boriding temperature and time (Ozbek *et al* 2002; Culha *et al* 2008; Sahin *et al* 2010), hardness of the boride layer increased due to the FeB phase.

Tabur *et al* (2009) pack borided AISI 8620 steel at temperatures of 1123, 1173, and 1223 K for 2, 4 and 6 h and they found that the surface hardness of boriding steel was 1650 and 1860 $HV_{0.1}$ for 2 h at 1123 and 1223 K for 6 h, respectively. The boride layer hardness obtained as a result of the plasma paste boriding process in lower temperatures and in shorter time was found to be higher compared with the hardness values obtained by traditional boriding (Genel *et al* 2003; Genel 2006; Ozbek *et al* 2002) methods.
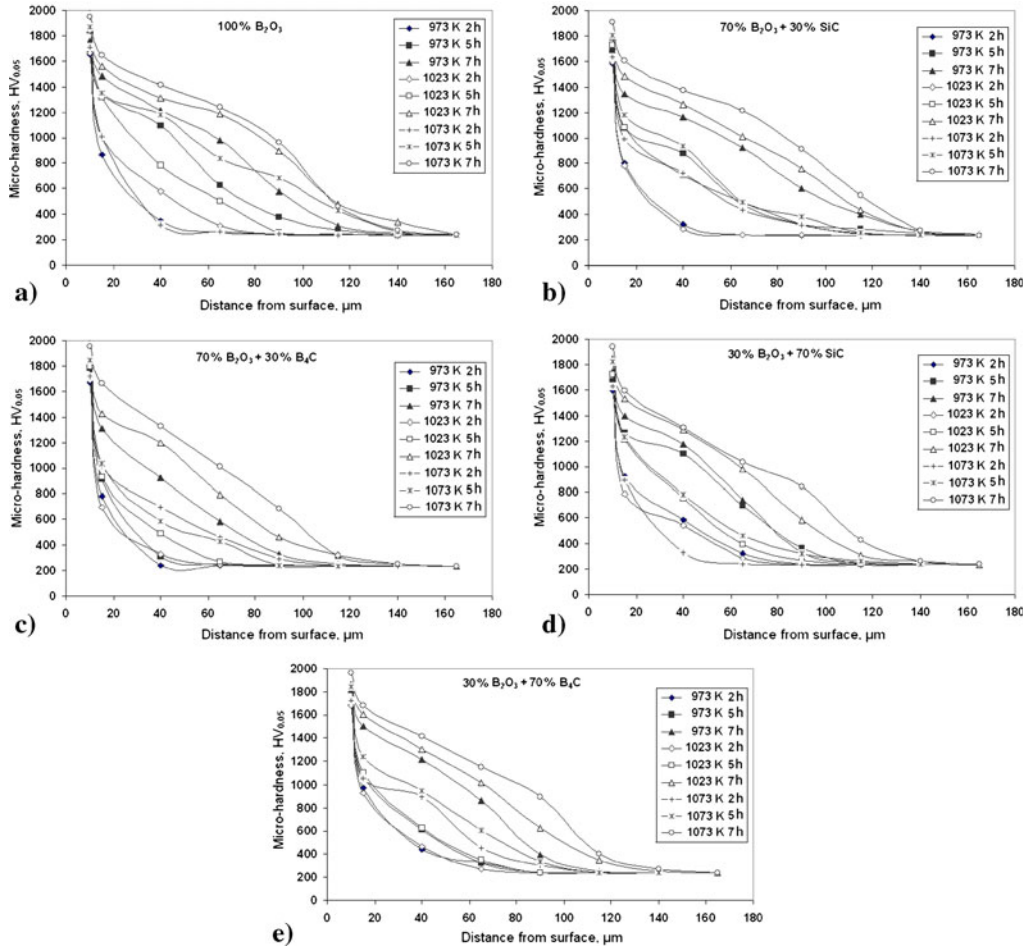
Figure 4. From surface to core hardness distribution of the steel plasma paste borided in different % B_2O_3 paste mixtures, **a**) 100 B_2O_3, **b**) 70 B_2O_3 + 30 SiC, **c**) 70 B_2O_3 + 30 B_4C, **d**) 30 B_2O_3 + 70 SiC, **e**) 30 B_2O_3 + 70 B_4C.

3.3 *Kinetics*

There is a parabolic relationship between boride layer thickness and boriding time. As can be seen in figure 5, there is a variation of boriding layer thickness with time at different temperatures. The thickness of the boride layer as a function of squared time is described by:

$$x^2 = K.t, \tag{9}$$

where x is the depth of the boride layer, K is the growth rate constant, and t is the time. Generally, it is expected that the plot of boride layer thickness versus squared treatment time gives a straight line which indicates that the growth of the layer has a parabolic dependence to time. The values of K were calculated from the slopes of layer thickness versus squared treatment time graphs (figure 6). The relationship between the growth rate constant and the temperature can be
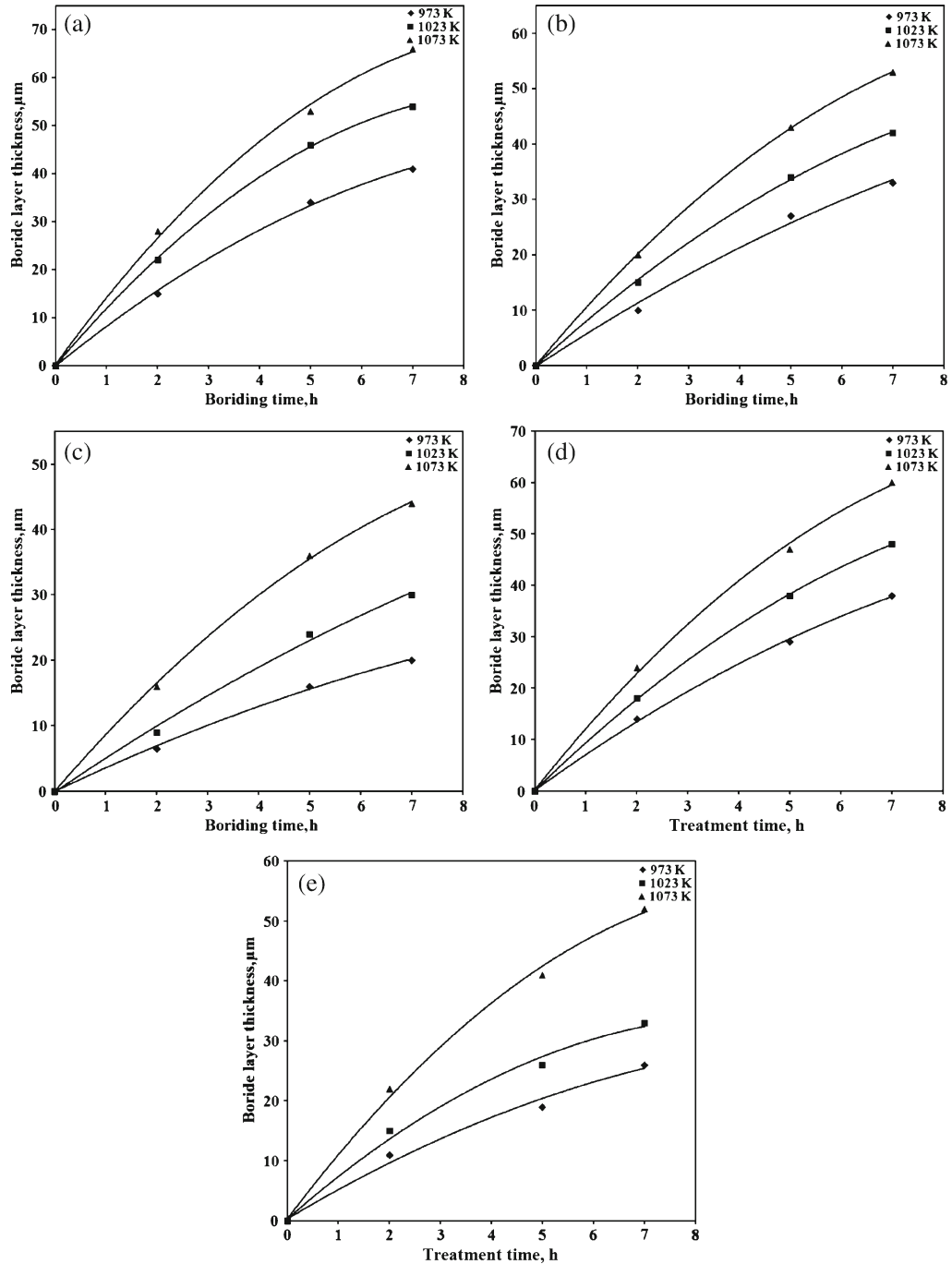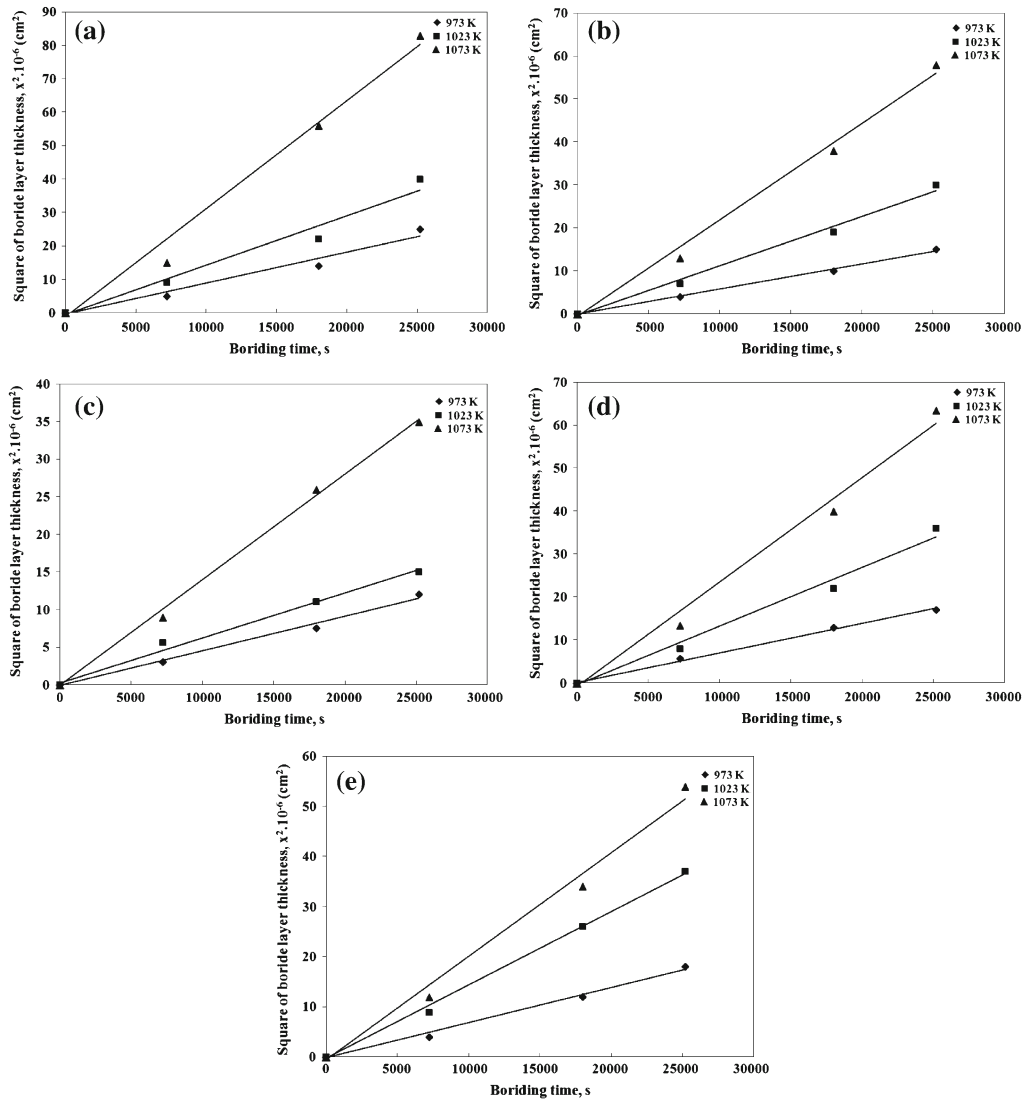
Figure 5. Variation of boriding layer thickness with time at different temperatures: **a**) 100 B_2O_3, **b**) 70 B_2O_3 + 30 SiC, **c**) 70 B_2O_3 + 30 B_4C, **d**) 30 B_2O_3 + 70 SiC, **e**) 30 B_2O_3 + 70 B_4C.

expressed by an Arrhenius type equation as

$$K = K_0 . \exp\left(-\frac{Q}{R.T}\right), \qquad (10)$$

where Q is the activation energy (J/mol); T is the absolute temperature (K) and R is the gas constant (J/mol K). Figure 6 is the plot of growth rate constant of the plasma paste boride layers in different B_2O_3% mixtures of the steel as a function of temperature. Consequently, the activation energy for the boron diffusion in the boride layer is determined by the slope obtained

Figure 6. Square of boride layer thickness in different % B_2O_3 mixtures versus boriding time at various temperatures for AISI 8620 steel: **a**) 100 B_2O_3, **b**) 70 B_2O_3 + 30 SiC, **c**) 70 B_2O_3 + 30 B_4C, **d**) 30 B_2O_3 + 70 SiC, **e**) 30 B_2O_3 + 70 B_4C.

by the plot of lnK vs. 1/T. Making use of the least squares analysis, the kinetics conclusions are obtained as

$$K_{B_2O_3} = K_0.\exp\left(-\frac{124716}{R.T}\right), \tag{11}$$

$$K_{70\%B_2O_3+30\%SiC} = K_0.\exp\left(-\frac{129336}{R.T}\right), \tag{12}$$

$$K_{70\%B_2O_3+30\%B_4C} = K_0.\exp\left(-\frac{138574}{R.T}\right), \tag{13}$$

$$K_{30\%B_2O_3+70\%SiC} = K_0.\exp\left(-\frac{126564}{R.T}\right), \tag{14}$$

$$K_{30\%B_2O_3+70\%B_4C} = K_0.\exp\left(-\frac{131183}{R.T}\right). \tag{15}$$

for the temperature range of 973 K to 1073 K. Table 2 shows the growth rate constant (K) and activation energy (Q) as a function of boriding temperature and on the samples borided with different $B_2O_3\%$ paste mixture. Together with the increase in temperature from 973 K to 1073 K, an increase occurred in the diffusion coefficient values of boron in the boride layer. Since the diffusion process speeds up along with the increase in temperature, boride layers were obtained. The diffusion coefficient for the samples borided with B_2O_3 paste with SiC and B_4C were observed to have decreased the diffusion coefficient. Lower diffusion coefficient values were established in the B_4C addition compared with the SiC addition. B_4C did not contribute much since the plasma paste boriding process was conducted in the lower temperatures of 973 and 1023 K. However, with the temperature increased to 1073 K, B_4C was found to have contributed to the boriding treatment. While the highest activation energy was observed as 138.574 kJ/mol in 70% B_2O_3 + 30% B_4C paste, the lowest was obtained from 100% B_2O_3 paste as 124.716 kJ/mol. The addition of B_4C and SiC to B_2O_3 paste increased the activation energy values. Kartal *et al* (2011) borided low carbon steel by electrochemical boriding. They reported that using the electrochemical boriding process, the activation energy was determined to be 172.75 ± 8.6 kJ/mol. Obviously, a significant decrease (i.e., ≈28%) in Q is feasible with plasma paste boriding methods.

Diffusion coefficient values obtained through plasma paste boriding methods were established as higher compared with the traditional boriding methods. At the end of plasma paste boriding,

Table 2. Growth rate constant (K) and activation energy (Q) as a function of boriding temperature and steel.

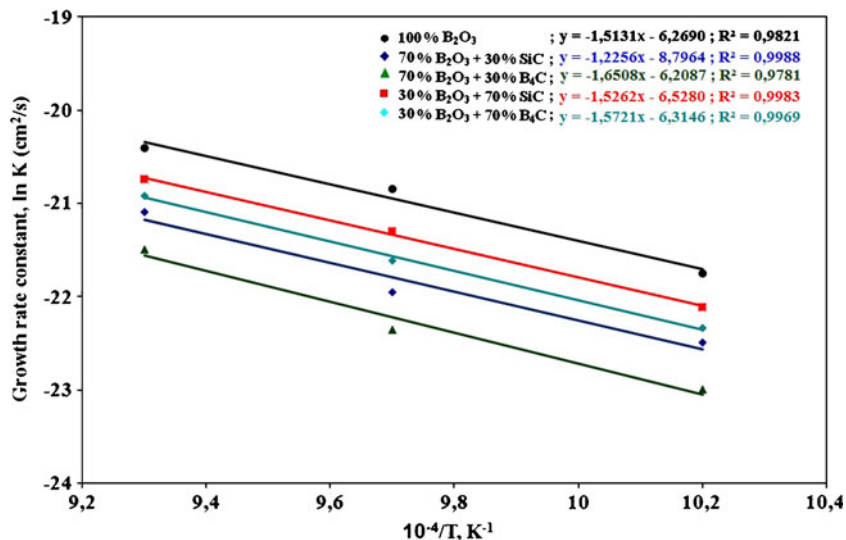| | Growth rate constant ($cm^2\ s^{-1}$) | | | |
| | Temperature, K | | | Activation energy |
Steel	973	1023	1073	(kJ/mol)
100% B_2O_3	$3,82.\ 10^{-10}$	$8,11.\ 10^{-10}$	$16,07.\ 10^{-10}$	124.716
70% B_2O_3 + 30% SiC	$0.18.\ 10^{-10}$	$0,37.\ 10^{-10}$	$0,76.\ 10^{-10}$	129.336
70% B_2O_3 + 30% B_4C	$0,73.\ 10^{-10}$	$1,69.\ 10^{-10}$	$3,61.\ 10^{-10}$	138.574
30% B_2O_3 + 70% SiC	$2,34.\ 10^{-10}$	$5,04.\ 10^{-10}$	$10,08.\ 10^{-10}$	126.564
30% B_2O_3 + 70% B_4C	$1,64.\ 10^{-10}$	$3,62.\ 10^{-10}$	$7,43.\ 10^{-10}$	131.183

Table 3. The comparison of activation energy for diffusion of boron with respect to the different boriding medium and steel.

Steel	Temperature range (K)	Boriding medium	Activation energy (kJ/mol)	References
Mild steel	973–1273	Spark Plasma Sintering (SPS)	145.8	Yu *et al* (2002)
Low carbon steel	1123–1273	Electrochemical	172.75	Kartal *et al* (2011)
AISI W1	1123–1323	Salt bath	171.2	Genel *et al* (2003)
AISI 4340	1073–1273	Salt bath	234	Sen *et al* (2005a)
AISI 304	1073–1223	Salt bath	253.3	Taktak (2006)
AISI 1045	1193–1273	Solid	226.7	Campos *et al* (2005)
AISI 4140	1123–1223	Solid	215	Sen *et al* (2005b)
34CrAlNi7	1123–1223	Solid	270	Efe *et al* (2008)
AISI 316	1073–1223	Solid	199	Ozdemir *et al* (2008)
AISI 8620	973–1073	Plasma paste (B_2O_3 based pastes)	124.7–138.5	Present study

diffusion coefficient values were observed to change in the range of $0{,}18 \times 10^{-10}$ and $16{,}07 \times 10^{-10}$. The calculated diffusion coefficient of the present study is in good agreement with values reported in the literature (Oliveria *et al* 2010; Sen *et al* 2005a, b; Taktak 2006).

The kinetics results of the present study are effectively comparable with references (Yu *et al* 2002; Kartal *et al* 2011; Genel *et al* 2003; Sen *et al* 2005a, b; Taktak 2006; Campos *et al* 2005; Efe *et al* 2008; Ozdemir *et al* 2008) as seen in table 3. Activation energy values obtained through the plasma paste boriding % method were established as lower compared with other boriding methods (Yu *et al* 2002; Kartal *et al* 2011; Genel *et al* 2003; Sen *et al* 2005a, b; Taktak 2006; Campos *et al* 2005; Efe *et al* 2008; Ozdemir *et al* 2008). Yoon *et al* (1999) borided AISI 304 steel by plasma paste which consisted of borax ($Na_2B_4O_7$) and amorphous boron, at different temperatures in Ar/H_2 gases and examined the diffusion kinetics and morphology of the layer.

Figure 7. Growth rate constant vs. temperature of % B_2O_3 paste mixtures of plasma paste borided the steel and correlation coefficients (R^2).

They reported that using the plasma paste process caused lower activation energy for the formation of the boride layer than that of conventional boriding processes. The calculated activation energy of the present study is in good agreement with values reported in the literature (Sen *et al* 2005a, b; Taktak 2006; Campos *et al* 2005; Efe *et al* 2008; Ozdemir *et al* 2008).

Figure 7 illustrates lnK-1/T graphics and correlation coefficient values of cementation steel that was plasma paste borided in different $B_2O_3\%$ paste mixture. Correlation coefficients indicate the degree of reliability of the predicted results, when compared with that of the experiments. The closer the values of the correlation coefficients to 1, the more reliable are the calculated results with respect to the experiment. Therefore, utilization of those equations is of importance in predicting process results for practical applications as well as scientific studies (Sen *et al* 2005a, b).

4. Conclusions

The AISI 8620 steel was successfully paste borided in 70% H_2–30% Ar gas mixture plasma at temperatures of 973, 1023 and 1073 K for 2, 5 and 7 h with various B_2O_3 paste mixture. It is possible to boride steels using B_2O_3 based pastes at low temperatures in plasma that activates the chemical reactions. A double phase pattern (FeB + Fe_2B) was obtained after plasma paste boriding as a result of X-ray diffraction analysis. While the lowest hardness obtained was 1583 $HV_{0.05}$ for 70% B_2O_3 + 30% SiC paste mixture for 2 h at 973 K, the highest hardness found was 1992 $HV_{0.05}$ for 30% B_2O_3 + 70% B_4C paste for 7 h at 1073 K. Activation energy values obtained through plasma paste boriding with $B_2O_3\%$ paste mixture were established as lower compared with other boriding methods. While the highest activation energy was found as 138.574 kJ/mol in 70% B_2O_3 + 30% B_4C paste, the lowest was obtained as 124.716 kJ/mol in 100% B_2O_3 paste.

Acknowledgements

References

Bartsch K & Leonhardt A 1999 Formation of iron boride layers on steel by d.c.-plasma boriding and deposition processes. *Surf. Coat Technol.* 116(119): 386–390

Bejar M A & Henríquez R 2009 Surface hardening of steel by plasma- electrolysis boronizing. *Mater. Des.* 30: 1726–1728

Bindal C & Ucisik A H 1999 Characterization of borides formed on impurity-controlled chromium-based low alloy steels. *Surf. Coat Technol.* 122: 208–213

Buijnsters J G, Shankar P, Gopalakrishnan P, Van Enckevort W J P, Schermer J J, Ramakrishnan S S and Ter Meulen J J 2003 Diffusion-modified boride interlayers for chemical vapour deposition of low-residual-stress diamond films on steel substrates. *Thin Solid Films.* 426: 85–93

Campos I, Bautista O, Ramírez G, Islas M, de la Parra J and Zuñiga L 2005 Effect of boron paste thickness on the growth kinetics of Fe_2B boride layers during the boriding process. *Appl. Surf. Sci.* 243: 429–436

Chen X J, Yu L G, Khor K A and Sundararajan G 2008 The effect of boron-pack refreshment on the boriding of mild steel by the spark plasma sintering (SPS) process. *Surf. Coat. Technol.* 202: 2830–2836

Culha O, Toparli M, Sahin S and Aksoy T 2008 Characterization and determination of Fe$_x$B layers' mechanical properties. *Mater. Proces. Technol.* 206: 231–240

Davis J A, Wilbur P J, Williamson D L, Wei R and Vajo J J 1998 Ion implantation boriding of iron and AISI M2 steel using a high-current density, low energy, broad-beam ion source. *Surf. Coat. Technol.* 103–104: 52–57

Dong M, Bao-luo S and Xin Z 2010 Effects of boronizing on mechanical and dry-sliding wear properties of CoCrMo alloy. *Mater. Des.* 31: 3933–3936

Efe G C, Ipek M, Ozbek I and Bindal C 2008 Kinetics of borided 31CrMoV9 and 34CrAlNi7 steels. *Mater. Charact.* 59: 23–31

Genel K 2006 Boriding kinetics of H13 steel. *Vacuum.* 80: 451–457

Genel K, Ozbek I and Bindal C 2003 Kinetics of boriding of AISI W1 steel. *Mater. Sci. and Eng. A.* 347: 311–314

Gunes I, Ulker S and Taktak S 2011 Plasma paste boronizing of AISI 8620, 52100 and 440C steels. *Mater. Des.* 32: 2380–2386

Kartal G, Eryilmaz O L, Krumdick G, Erdemir A and Timur S 2011 Kinetics of electrochemical boriding of low carbon steel. *Appl. Surf. Sci.* 257: 6928–6934

Khor K A, Yu L G and Sundararajan G 2005 Formation of hard tungsten boride layer by spark plasma sintering boriding. *Thin Solid Films.* 478: 232–237

Kayali Y, Gunes I and Ulu S 2012 Diffusion kinetics of borided AISI 52100 and AISI 440C steels. *Vacuum.* 86: 1428–1434

Lou D C, Solberg J K, Akselsen O M and Dahl N 2009 Microstructure, property investigation of paste boronized pure nickel, Nimonic 90 superalloy. *Mat. Chemistry and Phys.* 115: 239–244

Nam K S, Lee K H, Lee S R and Kwon S C 1998 A study on plasma-assisted boriding of steels. *Surf. Coat Technol.* 98: 886–890

Oliveria C K N, Casteletti L C, Lombardin Neto A, Totten G E and Heck S C 2010 Production and Characterization of Boride Layers on AISI D2 Tool Steel. *Vacuum.* 84: 792–796

Ozbek I, Konduk B A, Bindal C and Ucisik A H 2002 Characterization of borided AISI 316L stainless steel implant. *Vacuum.* 65: 521–525

Ozdemir O, Omar M A, Usta M, Zeytin S, Bindal C and Ucisik A H 2008 An investigation on boriding kinetics of AISI 316 stainless steel. *Vacuum.* 83: 175–179

Rodríguez C E, Laudien G, Biemer S, Rie K-T and Hoppe S 1999 Plasma-assisted boriding of industrial components in a pulsed d.c. glow discharge. *Surf. Coat Technol.* 116–119: 229–233

Sahin S, Meric C and Saritas S 2010 Production of ferroboron powders by solid boronizing method. *A Powder Technol.* 21: 483–487

Sen S, Ozbek I, Sen U and Bindal C 2001 Mechanical behavior of borides formed on borided cold work tool steel. *Surf. Coat Technol.* 135: 173–177

Sen S, Sen U and Bindal C 2005a An approach to kinetic study of borided steels. *Surf. Coat Technol.* 191: 274–85

Sen S, Sen U and Bindal C 2005b The growth kinetics of borides formed on boronized AISI 4140 steel. *Vacuum.* 77: 195–202

Shrivastava S, Jain A, Tarey RD, Avasthi DA, Kabiraj D, Senapati L and Mehta G K 1996 Hardening of steel by Boron Ion Implantation-Dependence on Phase Composition. *Vacuum.* 47: 247–249

Sinha A K 1991 Boronizing, ASM Handbook, *J. Heat Treat.*, USA

Tabur M, Izciler M, Gul F and Karacan I 2009 Abrasive wear behavior of boronized AISI 8620 steel. *Wear.* 266: 1106–1112

Taktak S 2006 A study on the diffusion kinetics of borides o boronized Cr-based steels. *J. Mater. Sci.* 41: 7590–7596

Torun O & Celikyurek I 2009 Boriding of diffusion bonded joints of pure nickel to commercially pure titanium. *Mater. Des.* 30: 1830–1834

Ulker S, Gunes I and Taktak S 2011 Investigation tribological behaviour of plasma paste boronized of AISI 8620, 52100 and 440C steels. *Indian J. Eng. Mater. Sci.* 18: 370–377

Yan P X, Wei Z Q, Wen X L, Wu Z G, Xu J W, Liu W M and Tian J 2002 Post boronizing ion implantation of C45 steel. *Appl. Surf. Sci.* 195: 74–79

Yoon J H, Jee Y K and Lee S Y 1999 Plasma paste boronizing treatment of the stainless steel AISI 304. *Surf. Coat. Technol.* 112: 71–75

Yu L G, Khor K A and Sundararajan G 2002 Boriding of mild steel using the spark plasma sintering (SPS) technique. *Surf. Coat. Technol.* 157: 226–230

Yu L G, Chen X J, Khor K A and Sundararajan G 2005 FeB/Fe$_2$B phase transformation during SPS pack-boriding: Boride layer growth kinetics. *Acta Mater.* 53: 2361–2368